Single Observer Geolocation for Periodic Communication Signals based on Doppler and TOA

Jinzhou Li, Shouye Lv, Chenglin Wang, Shuai Liao, Shaoqiong Zhou, Yang Liu
Key Laboratory of Spaceborne Information Intelligent Interpretation
Beijing Institute of Remote Sensing Information
Beijing, China, 100192
Email: lvshouye@126.com

***Abstract*—The disadvantages of single observer localization based on Doppler are poor geolocation accuracy and long cumulative time. Therefore, it is significant to improve geolocation accuracy without increasing the cost of payload. In this paper, the authors propose a single observer geolocation method for periodic communication signals based on Doppler and time delay. We first compare the Cramér-Rao lower bound (CRLB) differences with and without using time of arriving (TOA). CRLBs comparison shows the theoretical geolocation accuracy could be improved significantly by TOA for periodic signal. In the sequel we propose a maximum likelihood iterative geolocation approach. Simulation results show that the estimation accuracy approximately attains the CRLB and demonstrate the feasibility of the accuracy analysis.**

***Index Terms*—Doppler, TOA, Periodic communication signals, Single observer geolocation**

I. Introduction

Compared with multiple observers geolocation [1], [2], single observer position [3], [4], [5] does not need multi-station cooperative detection. Therefore, single observer geolocation is commonly used in the area of passive location. Commonly used signal measurements for single observer position include time of arrive (TOA) [6], [7], angle of arrival (AOA) [8], [9] Doppler [10] and interferometer phase difference [11]. Most localization schemes with TOA deal with cooperative sensors with known synchronization protocols between transmitter and receivers. High precision of AOA depends on multi-channel phase interferometers [12], [13] which will increase the cost of receiver payload. Therefore, single observer geolocation based on Doppler is widely used in the area of passive localization. However, The disadvantages of single observer geolocation based on Doppler are poor localization precision and long cumulative time. It is significant that how to improve localization accuracy without increasing the cost of observer.

In practical application, there are some special communication signals with constant period such as Link-4A and Demand-Assigned-Multiple-Access (DAMA). Tzoreff et al. [14] discussed passive localization with single observer based on TOA measurements only. The authors also analyzed the effects of imprecise signal period because of oscillator instability. In this paper, we focus on the scene of single observer geolocation based on Doppler. The TOA information is adopted when the signal is periodic with known constant period.

Section II provides mathematical formulation of the geolocation scene. In section III we develop the CRLBs for the emitter geolocation with and without using TOA information. Section IV presents the Maximum likelihood (ML) iterative estimator of the emitter location based on Doppler and TOA. Section V provides simulation results including mean square error (MSE) and CRLB results for the localization performance. Finally, Section VI concludes the paper.

II. Problem Formulation

Consider a stationary emitter at $\mathbf{u}^o$ and a moving receiver whose initial position is $\mathbf{s}_1$. For simplicity, the receiver velocity $\mathbf{v}$ is assumed to be fixed during the whole observation interval. The period T_p of signal transmitted by the emitter is known and constant. Suppose the receiver attains M chip periodic signals. In practical application, there are many types of communication signal with constant period. For example, Fig. 1 shows the DAMA signals which are commonly used in UHF Follow-on (UFO) communications satellite.

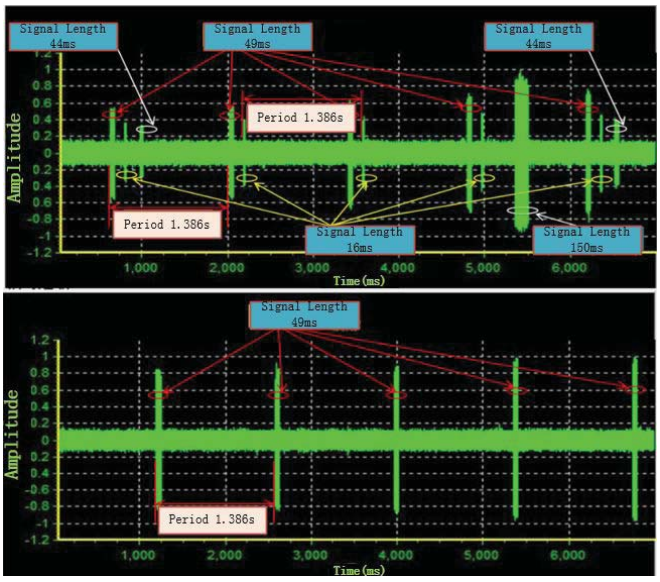

Fig. 1. The periodic signals of UFO communications satellite

The TOA and Doppler of the i^{th} chip signal are t_i^o and f_i^o.

$$t_i^o = t_0 + \frac{1}{c}\left\|\mathbf{u}^o - \mathbf{s}_i\right\| + (i-1)\,T_p, i = 1, ..., M \quad (1)$$

$$f_i^o = f_0\left[1 - \frac{\mathbf{v}^T\left(\mathbf{s}_i - \mathbf{u}^o\right)}{c\left\|\mathbf{s}_i - \mathbf{u}^o\right\|}\right], i = 1, ..., M \quad (2)$$

where t_0 is the transmitted time of the first chip signal. c is the signal propagation speed. f_0 is the original carrier frequency. $\mathbf{s}_i$ is the receiver position when observed the i^{th} chip signal.

$$\mathbf{s}_i = \mathbf{s}_1 + (i-1)\,T_p\mathbf{v} \quad (3)$$

The TOA and Doppler measurements are $t_i = t_i^o + \Delta t_i$ and $f_i = f_i^o + \Delta f_i$, where Δt_i and Δf_i are Gaussian noises.

$$\mathbf{t} = \left[\begin{array}{cccc} t_1 & t_2 & \cdots & t_M \end{array}\right]^T = \mathbf{t}^o + \Delta\mathbf{t} \quad (4)$$

$$\mathbf{f} = \left[\begin{array}{cccc} f_1 & f_2 & \cdots & f_M \end{array}\right]^T = \mathbf{f}^o + \Delta\mathbf{f} \quad (5)$$

where

$$\mathbf{t}^o = \left[\begin{array}{cccc} t_1^o & t_2^o & \cdots & t_M^o \end{array}\right]^T$$

$$\Delta\mathbf{t} = \left[\begin{array}{cccc} \Delta t_1 & \Delta t_2 & \cdots & \Delta t_M \end{array}\right]^T$$

$$\mathbf{f}^o = \left[\begin{array}{cccc} f_1^o & f_2^o & \cdots & f_M^o \end{array}\right]^T$$

$$\Delta\mathbf{f} = \left[\begin{array}{cccc} \Delta f_1 & \Delta f_2 & \cdots & \Delta f_M \end{array}\right]^T$$

The TOA and Doppler measurement errors $\Delta\mathbf{t}$ and $\Delta\mathbf{f}$ are zero-mean and statistically independent Gaussian random vector with covariance matrices $E\left[\Delta\mathbf{t}\Delta\mathbf{t}^T\right] = \mathbf{Q}_t$ and $E\left[\Delta\mathbf{f}\Delta\mathbf{f}^T\right] = \mathbf{Q}_f$.

If the transmitted signal is aperiodic, the emitted time is unknown. TOA information t_i is unusable for single observer geolocation. Therefore, single observer geolocation based on Doppler is widely used in this scene. For the case of periodic signal, the transmitted time of each chip signal is $t_0 + (i-1)\,T_p$ with constant known interval T_p. The unknown original emitted time t_0 could be eliminated by TOAs difference. Therefore, TOA information could be used to improved geolocation accuracy for periodic signal.

III. CRLB AND PERFORMANCE ANALYSIS

A. CRLB

CRLB defines the best accuracy that an unbiased estimator could achieve. This section derives the CRLB of single receiver geolocation based on Doppler only and the CRLB of using Doppler and TOA. Then the differences of the CRLBs are compared to indicate the increasement of using TOA information. The TOA measurements $\mathbf{t}$ could be transformed as $\mathbf{d}_t = \mathbf{A}\mathbf{t}$ which will eliminate the unknown variable t_0. The covariance matrix of $\Delta\mathbf{d}_t$ could be expressed as $\mathbf{Q}_d = \mathbf{A}\mathbf{Q}_t\mathbf{A}^T$, where

$$\mathbf{A} = \left[\begin{array}{cccccc} -1 & 1 & 0 & \cdots & 0 & 0 \\ 0 & -1 & 1 & \cdots & 0 & 0 \\ 0 & 0 & -1 & \cdots & 0 & 0 \\ \vdots & \vdots & \vdots & \vdots & \vdots & \vdots \\ 0 & 0 & 0 & \cdots & -1 & 1 \end{array}\right]_{(M-1)\times M} \quad (6)$$

Define the unknown parameter vector $\theta = \left[\mathbf{u}^{oT}, f_o\right]^T$ and the measurement parameter vector $\mathbf{\Phi} = \left[\mathbf{d}_t^T, \mathbf{f}^T\right]^T$, the logarithm of the probability density function is

$$\begin{aligned} \ln P\left(\mathbf{\Phi}, \theta\right) &= \ln P\left(\mathbf{d}_t, \theta\right) + \ln P\left(\mathbf{f}, \theta\right) \\ &= K_1 + K_2 - \frac{1}{2}(\mathbf{d}_t - \mathbf{d}_t^o)^T\mathbf{Q}_d^{-1}\left(\mathbf{d}_t - \mathbf{d}_t^o\right) \\ &\quad - \frac{1}{2}(\mathbf{f} - \mathbf{f}^o)^T\mathbf{Q}_f^{-1}\left(\mathbf{f} - \mathbf{f}^o\right) \end{aligned} \quad (7)$$

where K_1 and K_2 are constants and independent of θ. Applying partial derivatives with respect to the unknown parameter twice yields

$$CRLB\left(\theta\right) = -E\left[\frac{\partial^2 \ln P\left(\mathbf{\Phi}, \theta\right)}{\partial\theta\partial\theta^T}\right] = \left[\begin{array}{cc} \mathbf{X} & \mathbf{Y} \\ \mathbf{Y}^T & \mathbf{Z} \end{array}\right]^{-1} \quad (8)$$

where

$$\begin{aligned} \mathbf{X} = &\left(\frac{\partial\mathbf{d}_t}{\partial\mathbf{u}}\right)^T\left(\mathbf{A}\mathbf{Q}_t\mathbf{A}^T\right)^{-1}\left(\frac{\partial\mathbf{d}_t}{\partial\mathbf{u}}\right) \\ &+ \left(\frac{\partial\mathbf{f}}{\partial\mathbf{u}}\right)^T\mathbf{Q}_f^{-1}\left(\frac{\partial\mathbf{f}}{\partial\mathbf{u}}\right) \end{aligned} \quad (9)$$

$$\mathbf{Y} = \left(\frac{\partial\mathbf{f}}{\partial\mathbf{u}}\right)^T\mathbf{Q}_f^{-1}\left(\frac{\partial\mathbf{f}}{\partial f_o}\right) \quad (10)$$

$$\mathbf{Z} = \left(\frac{\partial\mathbf{f}}{\partial f_o}\right)^T\mathbf{Q}_f^{-1}\left(\frac{\partial\mathbf{f}}{\partial f_o}\right) \quad (11)$$

$$\frac{\partial\mathbf{d}_t}{\partial\mathbf{u}} = \left[\begin{array}{ccc} \frac{\partial t_2}{\partial\mathbf{u}} - \frac{\partial t_1}{\partial\mathbf{u}} & \cdots & \frac{\partial t_M}{\partial\mathbf{u}} - \frac{\partial t_{M-1}}{\partial\mathbf{u}} \end{array}\right] \quad (12)$$

$$\frac{\partial\mathbf{f}}{\partial\mathbf{u}} = \left[\begin{array}{ccc} \frac{\partial f_1}{\partial\mathbf{u}} & \cdots & \frac{\partial f_M}{\partial\mathbf{u}} \end{array}\right] \quad (13)$$

$$\frac{\partial\mathbf{f}}{\partial f_o} = \left[\begin{array}{ccc} \frac{\partial f_1}{\partial f_o} & \cdots & \frac{\partial f_M}{\partial f_o} \end{array}\right]^T \quad (14)$$

$$\frac{\partial t_i}{\partial\mathbf{u}} = \frac{\mathbf{u} - \mathbf{s}_i}{c\left\|\mathbf{u} - \mathbf{s}_i\right\|} \quad (15)$$

$$\frac{\partial f_i}{\partial\mathbf{u}} = \frac{f_o}{c}\left[\frac{\mathbf{v}}{\left\|\mathbf{u} - \mathbf{s}_i\right\|} - \frac{\left(\mathbf{s}_i - \mathbf{u}\right)^T\mathbf{v}\left(\mathbf{s}_i - \mathbf{u}\right)}{\left\|\mathbf{u} - \mathbf{s}_i\right\|^3}\right] \quad (16)$$

$$\frac{\partial f_i}{\partial f_o} = 1 - \frac{\mathbf{v}^T\left(\mathbf{s}_i - \mathbf{u}^o\right)}{c\left\|\mathbf{s}_i - \mathbf{u}^o\right\|} \quad (17)$$

Applying the partitioned matrix inversion formula [15] to (8) yields

$$CRLB_1\left(\mathbf{u}\right) = \mathbf{X}^{-1} + \mathbf{X}^{-1}\mathbf{Y}(\mathbf{Z} - \mathbf{Y}^T\mathbf{X}^{-1}\mathbf{Y})^{-1}\mathbf{Y}^T\mathbf{X}^{-1} \quad (18)$$

With similar derivations, the CRLB of the emitter position based on Doppler only can be shown as

$$CRLB_o\left(\mathbf{u}\right) = \mathbf{X}_o^{-1} + \mathbf{X}_o^{-1}\mathbf{Y}(\mathbf{Z} - \mathbf{Y}^T\mathbf{X}_o^{-1}\mathbf{Y})^{-1}\mathbf{Y}^T\mathbf{X}_o^{-1} \quad (19)$$

where

$$\mathbf{X}_o = \left(\frac{\partial\mathbf{f}}{\partial\mathbf{u}}\right)^T\mathbf{Q}_f^{-1}\left(\frac{\partial\mathbf{f}}{\partial\mathbf{u}}\right) \quad (20)$$

B. Performance comparison of CRLBs

The simulations discussed hereafter focus on 2-dimension scene, and the simulation for 3-dimension case is similar. Since the position and velocity of the receiver are known. The motion type of the receiver does not affect simulation results. For simplicity, we assume the receiver moves on a straight line with initial position $\mathbf{s}_1 = [300, 100]^T$m and velocity $\mathbf{v} = [300, -20]^T$m/s. The stationary emitter location is $\mathbf{u}^o = [2000, 2500]^T$m. The transmitted period is stationary and known with $T_p = 1.386$s. In Figs. 2 and 3, the cumulative time is 138.6s, and the receiver obtains $M = 100$ chips of signals. In Fig. 4, the cumulative time is a varying parameter. $\mathbf{Q}_t$ and $\mathbf{Q}_f$ are $M \times M$ diagonal matrix with elements σ_t^2 and σ_f^2 respectively.

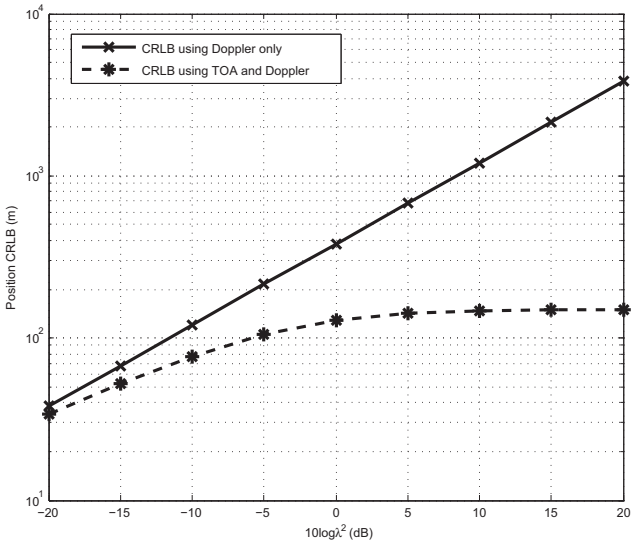

Fig. 2. Comparison of geolocation CRLBs by varying Doppler errors

In the first experiment, we examine the effect of Doppler measurement errors on the source localization by varying $\sigma_f = \lambda * 50Hz$. The TOA measurement errors is fixed at $\sigma_t = 500ns$. It can be seen from Fig. 2 that the periodic TOA information could improve the localization precision significantly from the CRLBs comparison. Note that as λ increasing, the effect of periodic TOA on the localization precision increases and therefore the difference between the CRLBs enlarges.

In the second experiment, we suppose the TOA and Doppler measurements are simultaneously affected by noise where $\sigma_f = \lambda * 50Hz$ and $\sigma_t = \lambda * 500ns$. Fig. 3 shows the theoretic localization improvement with the use of periodic TOA information. For example, the localization accuracy is about 381m for using Doppler only, and the accuracy is about 128m for the case of using both Doppler and TOA when the noise is $10 \log \lambda^2 = 0$.

In the third experiment, we examine the effect of cumulative time. Suppose the TOA and Doppler measurements noise are $\sigma_f = 50Hz$ and $\sigma_t = 500ns$ respectively. From Fig. 4, we

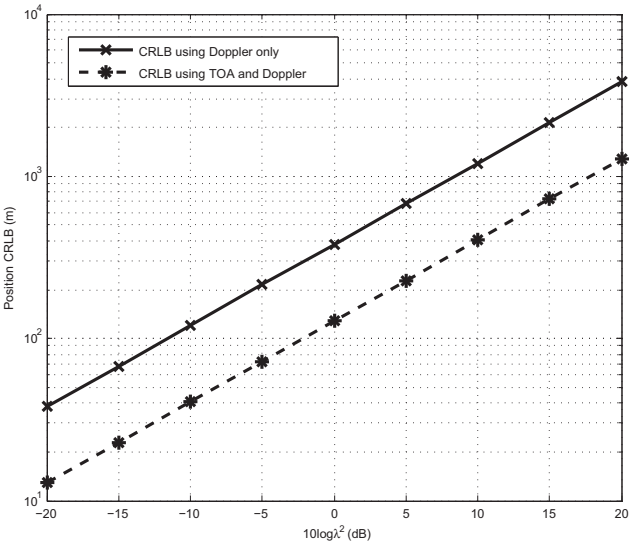

Fig. 3. Comparison of geolocation CRLBs by varying errors of both TOA and Doppler

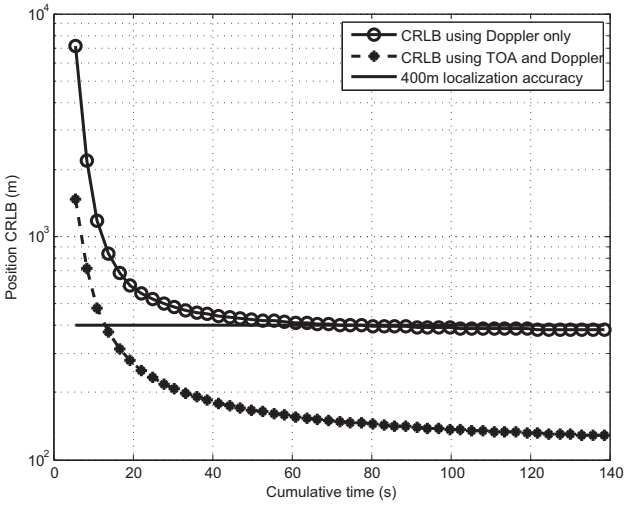

Fig. 4. Comparison of geolocation CRLBs by varying cumulative time

can find the algorithm of using Doppler only need about 80s cumulative time to attain 400m localization accuracy, which is less than 10s cumulative time for the method using Doppler and periodic TOA information.

IV. Maximum likelihood localization algorithms

A. Maximum likelihood estimator

This section first presents a maximum likelihood iterative estimator for the single observer geolocation based on TOA and Doppler. Then we give an iterative estimator based on Doppler only with similar derivations.

Let $\mathbf{\Phi} = \left[\mathbf{d}_i^T, \mathbf{f}^T\right]^T$ and $\theta = \left[\mathbf{u}^{oT}, f_o\right]^T$. $\theta_g = \left[\mathbf{u}_g^T, f_g\right]^T$ is a combination of initial source location and carrier frequency.

Then we have the approximation

$$\Delta\mathbf{\Phi} = \mathbf{\Phi} - \left(\mathbf{\Phi}|_{\theta=\theta_g}\right) - \left(\frac{\partial\mathbf{\Phi}}{\partial\theta}|_{\theta=\theta_g}\right)(\theta-\theta_g) \tag{21}$$

The least squares solution of $\delta\hat{\theta}$ is given by

$$\delta\hat{\theta} = \left[\left(\frac{\partial\mathbf{\Phi}}{\partial\theta}|_{\theta=\theta_g}\right)^T \mathbf{Q}_\Phi^{-1}\left(\frac{\partial\mathbf{\Phi}}{\partial\theta}|_{\theta=\theta_g}\right)\right]^{-1} * \left(\frac{\partial\mathbf{\Phi}}{\partial\theta}|_{\theta=\theta_g}\right)^T \mathbf{Q}_\Phi^{-1}(\theta-\theta_g) \tag{22}$$

where

$$\frac{\partial\mathbf{\Phi}}{\partial\theta}|_{\theta=\theta_g} = \begin{bmatrix} \frac{\partial\mathbf{d}_t^T}{\partial\mathbf{u}} & \frac{\partial\mathbf{f}^T}{\partial\mathbf{u}} \\ \mathbf{O} & \frac{\partial\mathbf{f}^T}{\partial f_o} \end{bmatrix}|_{\theta=\theta_g} \tag{23}$$

$$\mathbf{Q}_\Phi = \begin{bmatrix} \mathbf{A}\mathbf{Q}_t\mathbf{A}^T & \mathbf{O} \\ \mathbf{O} & \mathbf{Q}_f \end{bmatrix} \tag{24}$$

The corrected estimation $\theta^{(1)}$ is

$$\theta^{(1)} = \theta_g + \delta\hat{\theta} \tag{25}$$

The amended variable $\left\|\delta\hat{\theta}\right\|$ will converge to be smaller than threshold by multiple steps of iteration.Then $\theta^{(n)}$ is the finally estimation of the emitter position and carrier frequency.

The initial carrier frequency f_g is given by least square estimation.

$$f_g = \left(\frac{\partial\mathbf{f}}{\partial f_o}\right)^T \mathbf{f}\left(\left(\frac{\partial\mathbf{f}}{\partial f_o}\right)^T\left(\frac{\partial\mathbf{f}}{\partial f_o}\right)\right)^{-1} \tag{26}$$

The initial location $\mathbf{u}_g$ is easy to obtain by grid search around sub-satellite point with the cost function as follows.

$$Cost(\mathbf{u}) = \left\|\mathbf{f} - \hat{f}_k \cdot \left[\left(\frac{\partial\mathbf{f}}{\partial f_o}\right)\Big|_{\mathbf{u}=\mathbf{u}_k}\right]\right\|^2 \tag{27}$$

$$\hat{f}_k = \left(\frac{\partial\mathbf{f}}{\partial f_o}\right)^T \mathbf{f}\left(\left(\frac{\partial\mathbf{f}}{\partial f_o}\right)^T\left(\frac{\partial\mathbf{f}}{\partial f_o}\right)\right)^{-1}\Bigg|_{\mathbf{u}=\mathbf{u}_k} \tag{28}$$

where $\mathbf{u}_k$ is location of the k^{th} grid.

With similar derivations, the iterative estimator of geolocation based on Doppler only can be expressed as follows.

$$\delta\hat{\theta} = \left[\left(\frac{\partial\mathbf{f}}{\partial\theta}|_{\theta=\theta_g}\right)^T \mathbf{Q}_f^{-1}\left(\frac{\partial\mathbf{f}}{\partial\theta}|_{\theta=\theta_g}\right)\right]^{-1} * \left(\frac{\partial\mathbf{f}}{\partial\theta}|_{\theta=\theta_g}\right)^T \mathbf{Q}_f^{-1}(\theta-\theta_g) \tag{29}$$

B. Numerical Simulations

The performance of the proposed iterative solution is verified through simulation. The localization scene is the same as that in Section III. B. The estimate accuracy is defined as $MSE(\mathbf{u}) = \sum_{j=1}^{Num}\|\hat{\mathbf{u}} - \mathbf{u}^o\|^2 \Big/ Num$, where $Num = 500$ is the number of Monte Carlo runs. Each figure contains two sets of results. The first set of results shows the CRLB and MSE of the source estimation accuracy using Doppler only. The second set presents the CRLB and MSE of the source estimation accuracy using TOA and Doppler where signal is periodic with known period.

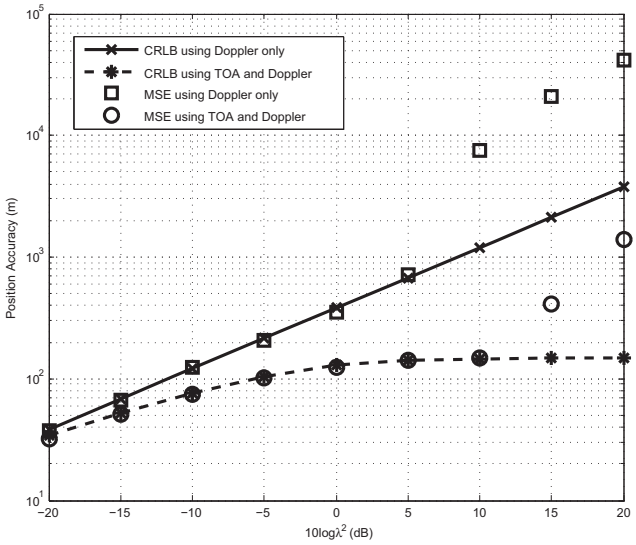

Fig. 5. Comparison of localization accuracy with the CRLB by varying Doppler errors

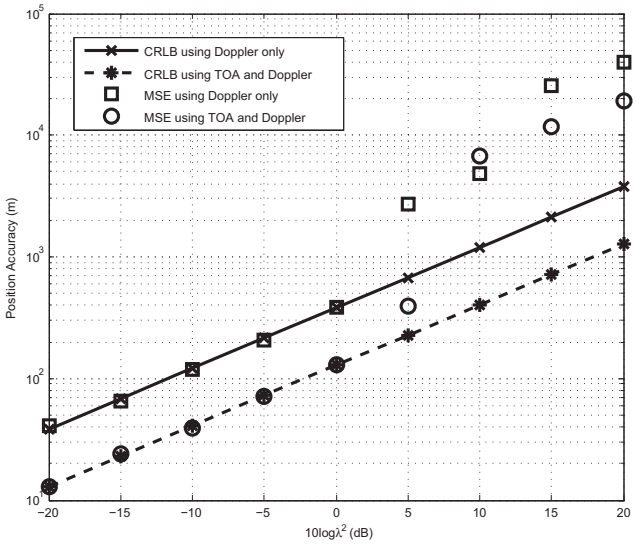

Fig. 6. Comparison of localization accuracy with the CRLB by varying errors of both TOA and Doppler

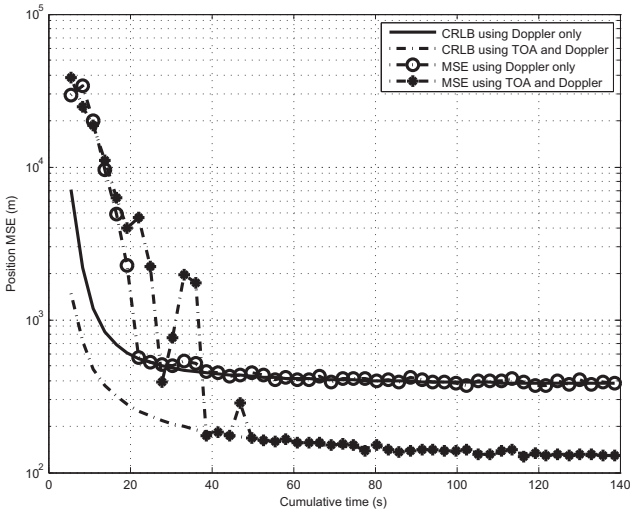

Fig. 7. Comparison of localization accuracy with the CRLB by varying cumulative time

In Fig. 5, we examine the effect of Doppler measurement errors on the source localization by varying $\sigma_f = \lambda * 50Hz$. The TOA measurement errors is fixed at $\sigma_t = 500ns$. The simulation results of both Maximum Likelihood (ML) iterative methods agree with the CRLBs very well when the Doppler measurement error λ is less than $10dB$.

Fig. 6 shows the performance of the Maximum Likelihood (ML) iterative algorithms by varying errors of both TOA and Doppler, where $\sigma_f = \lambda * 50Hz$ and $\sigma_t = \lambda * 500ns$. The improvement of localization accuracy is also obvious in Fig. 6 when measurement errors are small.

In Fig. 7, we examine the effect of cumulative time. The TOA and Doppler measurements noise are fixed at $\sigma_f = 50Hz$ and $\sigma_t = 500ns$. The localization accuracy will attain to 128m for using Doppler and TOA when the cumulative time is about 140s. However, the localization accuracy for the case of using Doppler only is about 385m.

V. Discussion and Conclusions

In this manuscript, we discussed the scene of single observer geolocaiton based on Doppler. The TOA measurements could be utilized to improve localization accuracy if the signal is periodic with known period. The CRLBs comparison proved that the performance improvement is significant. We also proposed iterative geolocation algorithms for the scene using Doppler only and the scene using both TOA and Doppler. The initial solutions of source position and carrier frequency are also provided. Finally, simulation results confirmed the theoretical development.

References

[1] J. L. Geeraert and J. W. McMahon, "Dual-satelite geolocation with ephemeris correction and uncertainty mapping," IEEE Transactions on Aerospace and Electronic Systems, vol. 56, no. 1, pp. 723-735, Feb. 2020.

[2] K. C. Ho, X. Lu, and L. Kovavisaruch, "Source localization using TDOA and FDOA measurements in the presence of receiver location errors: Analysis and solution," IEEE Transactions on Signal Process., vol. 55, no. 2, pp. 684-696, Feb. 2007.

[3] E. Tzoreff, B.Z. Bobrovsky, A.J. Weiss, "Single receiver emitter geolocation based on signal periodicity with oscillator instability," IEEE Transactions on Signal Process., vol.62, no.6, pp.1377-1385, Mar., 2014.

[4] G. Qi, Y. Li, et al., "An investigation on observer minimum circumnavigation velocity for bearings-only target tracking," IEEE Access, vol.8, pp. 126805-126813, 2020.

[5] F. Xiang, J. Wang and X. Yuan, "Research on passive detection and location by fixed single observer," 2020 International conference on information science, parallel and distributed systems (ISPDS), pp. 35-39, 2020.

[6] S. Zhao, N. Guo, et al., "Closed-form two-way TOA localization and synchronization for user devices with motion and clock drift," IEEE Signal Processing Letters, vol. 29, pp. 100-104, 2022.

[7] X. Li and K. Pahlavan, "Super-resolution TOA estimation with diversity for indoor geolocation," IEEE Transactions on Wireless Comm., vol. 3, no. 1, pp. 224-234, Jan. 2004.

[8] K. Hong, T. Wang, et al., "A learning-based AOA estimation method for device-free localization," IEEE Communications Letters, vol. 26, no. 6, pp. 1264-1267, June 2022.

[9] G. Wang, K. C. Ho and X. Chen, "Bias reduced semidefinite relaxation method for 3-D rigid body localization using AOA," IEEE Transactions on Signal Processing, vol. 69, pp. 3415-3430, 2021.

[10] R. Villalpando-Hernandez, D. Munoz-Rodriguez, C.Vargas-Rosarles and E. M. Avila, "Doppler position location: single observation point feasibility regions," IEEE Access, vol. 10, pp. 1802-1809, 2022.

[11] T. Zhou and Y. Cheng, "Research on High-Precision Extraction of Phase Difference Change Rate in Single Observer Passive Location," 2017 4th International Conference on Information Science and Control Engineering (ICISCE), pp. 1652-1655, 2017.

[12] J. Moghaddasi, T. Djerafi and K. Wu, "Multiport interferometer-enabled 2-D angle of arrival (AOA) estimation system," IEEE Transactions on Microwave Theory and Techniques, vol. 65, no. 5, pp. 1767-1779, May 2017.

[13] J. P. Younger and I. M. Reid, "Interferometer angle-of-arrival determination using precalculated phases," Radio Science, vol. 52, no. 9, pp. 1058-1066, Sept. 2017.

[14] E. Tzoreff, B.Z. Bobrovsky, A.J. Weiss, "Single receiver emitter geolocation based on signal periodicity with oscillator instability," IEEE Transactions On signal processing, vol.62, no.6, pp. 1377-1385, Mar. 2014.

[15] Marzetta, T. L. "A simple derivation of the constrained multiple parameter Cramer-Rao bound," IEEE Transactions on Acoustics, Speech and Signal Process., vol.41, no.6, pp. 2247-2249, June 1993.